

# Stable vapor-phase conversion of tetrahydrofurfuryl alcohol into 3,4-2H-dihydropyran

Satoshi Sato\*, Jun Igarashi, Yasuhiro Yamada

Graduate School of Engineering, Chiba University, Yayoi, Inage, Chiba 263-8522, Japan

## ARTICLE INFO

### Article history:

Received 12 October 2012

Received in revised form 1 December 2012

Accepted 8 December 2012

Available online 26 December 2012

### Keywords:

Dehydration

Tetrahydrofurfuryl alcohol

3,4-2H-dihydropyran

Alumina catalyst

Copper

Rhodium

Inhibition of coke formation

## ABSTRACT

Vapor-phase synthesis of 3,4-2H-dihydropyran (DHP) from tetrahydrofurfuryl alcohol (THFA) was investigated over acidic catalysts modified with transition metals. Catalytic activity of alumina was seriously deactivated in the reaction of THFA in nitrogen at 300 °C although the initial activity was high. Tetragonal ZrO<sub>2</sub> showed the catalytic activity to produce DHP at 350 °C. Alumina modified with Cu exhibits stable catalytic activity with high selectivity to DHP under hydrogen flow conditions, and the optimum activity was obtained at CuO contents of 5–10 wt.%; the selectivity to DHP was as high as 85%. Prior to the reaction, CuO was reduced to metallic Cu, which probably works as a product remover together with hydrogen to prevent coke formation. The reaction pathway from THFA to DHP was discussed: it is speculated that THFA is initially rearranged into 2-hydroxytetrahydropyran, which rapidly dehydrated to DHP.

© 2012 Elsevier B.V. All rights reserved.

## 1. Introduction

Biomass has the potential to serve as a sustainable chemical resource in the industrial society. In biorefinery development, various biomass-based chemicals have been listed as potential candidates of biorefinery building blocks, and furfural is expected as one of new candidates [1]. The new top 10 candidates are ethanol, furans including furfural, glycerol, biohydrocarbons including isoprene, lactic acid, succinic acid, hydroxypropionic acid/aldehyde, levulinic acid, sorbitol, and xylitol in this order. Furfural has been widely investigated on the catalytic conversion into useful chemicals, whereas the reports of furfural are much less than those of ethanol and glycerol.

Furfural with a low oxygen content is one of promising alternative chemical resources, and commercial production of furfural is well established [1]. Furfural is prepared through the dehydration of pentose polyols, such as xylose, or hemicelluloses catalyzed by sulfuric acid [2–4] and solid acid [5,6]. Hemicellulose, a polymer of glucose and xylose, is inedible biomass of some hardwoods and agriculture residues such as corncob and sugar cane bagasse [2]. Furfural can be derived to useful chemicals, such as furfuryl alcohol, tetrahydrofurfuryl alcohol (hereafter abbreviated as THFA), furfuryl

amine, furoic acid, 2-methylfuran, 2-methyltetrahydrofuran, furan, tetrahydrofuran [7–9], and cyclopentanone [10].

THFA can be obtained in the hydrogenation of furfural [8,11] and is used as an industrial solvent [9]. Various useful chemicals, such as  $\delta$ -valerolactone [12,13], tetrahydrofuran [13–16], 3,4-2H-dihydropyran (abbreviated as DHP) [17–26], 1,5-pentanediol [7,18,27–31], and 4-penten-1-ol [12,32–34], can be derived from THFA. In industrial applications, DHP is a chemical intermediate: it can be hydrated into 5-hydroxypentanal, which is further hydrogenated into 1,5-pentanediol [18]. DHP is also well known as a protection reagent of alcohol in organic synthesis [35].

It has been known that THFA is converted into DHP over alumina catalyst since 1930s (Fig. 1) [18]. The alumina catalyst, however, is readily deactivated in inert atmosphere such as N<sub>2</sub> and He flow, so that the yield of DHP is so high only in the initial period [17–19]. Several modifications of alumina with other metal oxides are found in patent literatures: TiO<sub>2</sub>-rich TiO<sub>2</sub>-Al<sub>2</sub>O<sub>3</sub> [20], V<sub>2</sub>O<sub>5</sub>/Al<sub>2</sub>O<sub>3</sub> [22], MoO<sub>3</sub>/Al<sub>2</sub>O<sub>3</sub> [22], and alumina catalysts modified with various metal oxides [23,24] work as a catalyst. It is reported that DHP yields exceed 90% at 250–320 °C [20,26], while the deactivation behavior is unclear. The catalyst needs regeneration process for the catalysts used in the reaction [20].

There are several reports on the inhibition of deterioration of acid-catalyzed reactions with the aid of supported noble metal in hydrogen gas [36–38]. We have also found that alumina modified by transition metals such as Co stabilizes the conversion of 3,3-dimethyl-2-butanone to produce 2,3-dimethyl-1,3-butadiene in H<sub>2</sub>

\* Corresponding author. Tel.: +81 43 290 3376; fax: +81 43 290 3401.  
E-mail address: [satoshi@faculty.chiba-u.jp](mailto:satoshi@faculty.chiba-u.jp) (S. Sato).

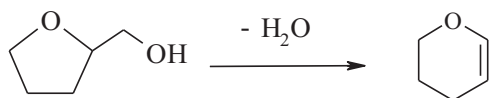


Fig. 1. Dehydration of THFA to DHP.

flow [39], whereas the catalytic activity of alumina is seriously deteriorated irrespective of its high initial activity. Hydrogen with the supported metal probably removes the product from the acid sites prior to coke formation and plays an important role to stabilize the catalytic activity of alumina.

In this paper, we investigated effective systems for the conversion of THFA into DHP to stabilize the catalytic activity and discussed the reaction pathway from THFA to DHP together with side reactions.

## 2. Experimental

### 2.1. Catalyst samples

THFA and DHP were purchased from Tokyo Chemical Industry Co. Ltd. 2-Hydroxytetrahydrofuran was synthesized via the hydration of DHP, according to a reference [40]. Metal nitrates such as  $\text{Co}(\text{NO}_3)_2$ ,  $\text{Ni}(\text{NO}_3)_2$ , and  $\text{Cu}(\text{NO}_3)_2$  were purchased from Wako Pure Chemical Industries Ltd. Alumina-supported noble metal catalysts, such as  $\text{M}/\text{Al}_2\text{O}_3$  ( $\text{M} = \text{Rh}, \text{Pt}, \text{Pd}$ ; 0.5 wt.%), were supplied by N.E. Chemcat Co.  $\gamma\text{-Al}_2\text{O}_3$  (DC-2382) and anatase  $\text{TiO}_2$  (DC-3124) were supplied by Dia Catalyst. Tetragonal  $\text{ZrO}_2$  (abbreviated as t- $\text{ZrO}_2$ ) was supplied by Saint-Gobain K. K. and monoclinic  $\text{ZrO}_2$  (m- $\text{ZrO}_2$ ) by Daichi Kigenso Kagaku Kogyo Co.  $\text{Yb}_2\text{O}_3$  and  $\text{La}_2\text{O}_3$  were supplied by Kanto Kagaku Co., Ltd.

Supported base-metal catalysts were prepared by impregnation using aqueous metal nitrate solution. The nitrate solution was added to a support, and water was evaporated at ambient pressure and  $70^\circ\text{C}$  by being illuminated by 350-W electric light bulb. After impregnation, the obtained solid was dried at  $110^\circ\text{C}$  over 24 h and then calcined at  $500^\circ\text{C}$  for 3 h.

### 2.2. Catalytic reaction

The reaction of THFA to DHP was performed in a fixed-bed down-flow glass tube reactor with an inner diameter of 17 mm and a length of 300 mm at  $200\text{--}300^\circ\text{C}$  under atmospheric pressure at  $\text{N}_2$ - or  $\text{H}_2$ -flow rate of  $20\text{ cm}^3\text{ min}^{-1}$ . Prior to the reaction, the catalyst was preheated in the carrier gas at  $500^\circ\text{C}$  for 1 h. After the preheating, the catalyst bed was cooled to the reaction temperature, and the substrate was fed into the reactor at a liquid feed rate of  $1.5\text{ cm}^3\text{ h}^{-1}$ . Unless otherwise noted, a reaction was carried out under the conditions using a catalyst of 0.5 g at  $300^\circ\text{C}$  and  $W/F = 0.32\text{ g h cm}^{-3}$ , where  $W$  and  $F$  are catalyst weight and reactant feed rate, respectively. The effluent was collected every hours for 5 h at  $0^\circ\text{C}$  and analyzed by FID-GC (GC-8A, Shimadzu Co.) using a 60-m capillary column of TC-WAX (GL Science Inc.). A GC-MS (QP5050A, Shimadzu Co.) was used to identify products in the effluent.

### 2.3. Characterization of catalyst

The specific surface area of the catalyst, SA, was calculated with the BET method using  $\text{N}_2$  isotherm at  $-196^\circ\text{C}$ . Thermogravimetry-differential thermal analysis (TG-DTA) was conducted in air using Thermo plus TG8120 (Rigaku Co.). Transmission electron microscopy (TEM) image was taken by a JEOL JEM-2100F microscope operated at 120 kV.

Table 1  
Physical and chemical properties of oxide catalysts.

Catalyst	SA ( $\text{m}^2\text{ g}^{-1}$ ) <sup>a</sup>	NH <sub>3</sub> desorption below $500^\circ\text{C}$ <sup>b</sup>	
		Peak ( $^\circ\text{C}$ )	Amount ( $\mu\text{mol g}^{-1}$ )
$\text{Al}_2\text{O}_3$	200	260	147
t- $\text{ZrO}_2$	179	262	108
m- $\text{ZrO}_2$	39	217	2
$\text{TiO}_2$	42	246	97

t- $\text{ZrO}_2$ , tetragonal  $\text{ZrO}_2$ ; m- $\text{ZrO}_2$ , monoclinic  $\text{ZrO}_2$ .

<sup>a</sup> Specific surface area.

<sup>b</sup> Calculated from TPD profiles in Fig. 2.

Temperature-programmed desorption (TPD) of  $\text{NH}_3$  adsorbed at  $100^\circ\text{C}$  was examined by neutralization titration using an electric conductivity cell immersed in aqueous  $\text{H}_2\text{SO}_4$  solution, and the detail procedure has been described elsewhere [41].  $\text{NH}_3$  that desorbed with  $\text{N}_2$  carrier gas was bubbled into a dilute  $\text{H}_2\text{SO}_4$  solution. The amount of desorbed  $\text{NH}_3$  was monitored from the change in conductivity of the solution. The sample was heated from 25 to  $800^\circ\text{C}$  at a rate of  $10^\circ\text{C min}^{-1}$  in  $\text{N}_2$  flow of  $50\text{ cm}^3\text{ min}^{-1}$ . The amount of acid sites is defined as the number of  $\text{NH}_3$  molecules desorbed in the temperature range of  $25\text{--}500^\circ\text{C}$  on the assumption that one  $\text{NH}_3$  molecule adsorbs on one basic site of the catalyst surface.

Temperature-programmed reduction (TPR) measurements were performed from 25 to  $900^\circ\text{C}$  at a heating rate of  $5\text{ K min}^{-1}$  to characterize the state of the supported metals. A mixture of  $\text{H}_2/\text{N}_2$  (=1/9) was flowed at a rate of  $10\text{ cm}^3\text{ min}^{-1}$  and ambient pressure over the catalyst filled in a quartz tube. The amount of  $\text{H}_2$  consumed during the reduction was monitored with a thermal conductivity detector.

## 3. Results and discussion

### 3.1. Characterization of catalyst samples

Table 1 summarized specific surface area of oxide catalysts such as  $\text{Al}_2\text{O}_3$ , t- $\text{ZrO}_2$ , m- $\text{ZrO}_2$  and  $\text{TiO}_2$ . Fig. 2 shows TPD profiles of  $\text{NH}_3$  adsorbed on the samples. The samples have desorption peak around  $250^\circ\text{C}$ . The amount of desorbed  $\text{NH}_3$  as a function of acid sites is also summarized in Table 1. Monoclinic  $\text{ZrO}_2$  was not acidic because  $\text{NH}_3$  did not adsorb at  $100^\circ\text{C}$ . It was proved that  $\text{Al}_2\text{O}_3$ , t- $\text{ZrO}_2$  and  $\text{TiO}_2$  were acidic, as it is well known.

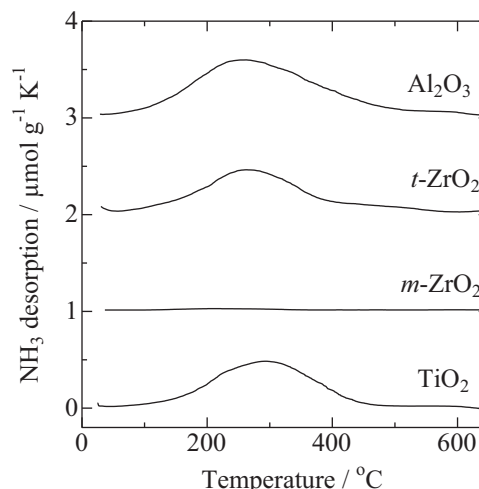
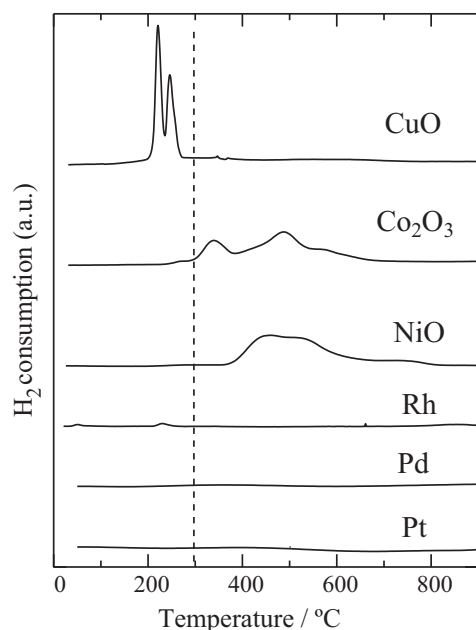


Fig. 2. TPD profiles of  $\text{NH}_3$  adsorbed on oxide catalysts.



**Fig. 3.** TPR profiles of Al<sub>2</sub>O<sub>3</sub>-supported metal catalysts. Metal loading, 15 wt.% for CuO, Co<sub>2</sub>O<sub>3</sub>, and NiO; 0.5 wt.% for Rh, Pd, and Pt.

Fig. 3 shows TPR profiles of alumina-supported metal oxides. Co<sub>3</sub>O<sub>4</sub>/Al<sub>2</sub>O<sub>3</sub> had reduction peaks at 339, 488, and 583 °C, and NiO/Al<sub>2</sub>O<sub>3</sub> had reduction peaks at 467 and 520 °C. CuO/Al<sub>2</sub>O<sub>3</sub> had reduction peaks at 221 and 246 °C. Rh/Al<sub>2</sub>O<sub>3</sub> had a very small reduction peak at 231 °C, while Pt/and Pd/Al<sub>2</sub>O<sub>3</sub> had no peaks. The TPR results indicate that the supported metals of CuO/Al<sub>2</sub>O<sub>3</sub>, Pd/Al<sub>2</sub>O<sub>3</sub>, Pt/Al<sub>2</sub>O<sub>3</sub>, and Rh/Al<sub>2</sub>O<sub>3</sub> are in metallic state in the reaction of THFA in H<sub>2</sub> flow at 300 °C. Fig. 4 shows a TEM image of 15 wt% CuO/Al<sub>2</sub>O<sub>3</sub> reduced at 500 °C. Bright particles of alumina with the size of 20–30 nm and dark copper particles with the same size as alumina were observed in the sample.

### 3.2. Reaction of THFA over several oxide catalysts

Table 2 summarizes the catalytic performance of several metal oxide catalysts in the dehydration of THFA at 300 or 350 °C in N<sub>2</sub> flow. DHP was produced over acid catalysts such as Al<sub>2</sub>O<sub>3</sub>, t-ZrO<sub>2</sub>, and TiO<sub>2</sub>, whereas DHP could not be produced over m-ZrO<sub>2</sub> and rare earth oxides such as Yb<sub>2</sub>O<sub>3</sub> and La<sub>2</sub>O<sub>3</sub>, which have only basic sites [42]. Catalytic activity of acidic Al<sub>2</sub>O<sub>3</sub> and t-ZrO<sub>2</sub> was significantly decreased with time on stream, as shown in Fig. 5A. TiO<sub>2</sub> also showed deterioration (figure not shown). In the acid catalysts, Al<sub>2</sub>O<sub>3</sub> and t-ZrO<sub>2</sub> showed moderate activity to DHP because the catalytic deactivation was occurred in 5 h. Thus, the results indicate that dehydration of THFA needs acidic sites. In addition, over

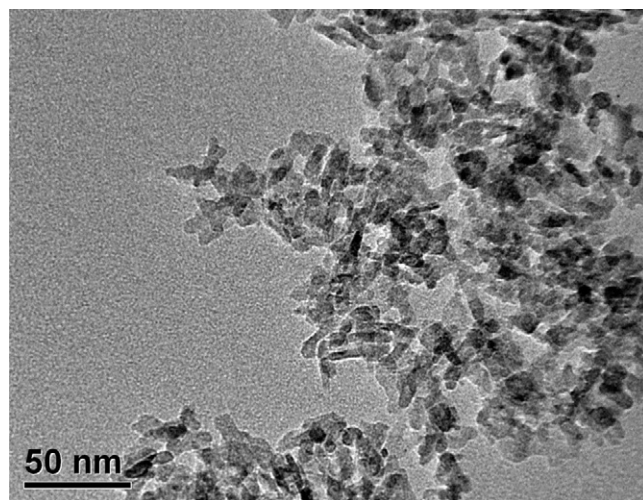


**Fig. 4.** TEM image of 10 wt% CuO/Al<sub>2</sub>O<sub>3</sub> reduced at 500 °C.

Al<sub>2</sub>O<sub>3</sub>, change in selectivity in H<sub>2</sub> flow was similar to that in N<sub>2</sub> flow (Fig. 5A).

### 3.3. Reaction of THFA over alumina catalysts modified with metals

Table 3 lists average catalytic activity of the samples in the initial 5 h. Commercial Rh/Al<sub>2</sub>O<sub>3</sub> and Pd/Al<sub>2</sub>O<sub>3</sub> used as a catalyst seemed to have moderate activity in N<sub>2</sub> flow at 300 °C. However, they were deteriorated with time on stream, as shown in blue dotted lines in Fig. 5B and C. The main product was DHP, and the by-products were tetrahydropyran and δ-valerolactone. In H<sub>2</sub> flow, however, Rh/Al<sub>2</sub>O<sub>3</sub> showed stable conversion of THFA (Fig. 5B), while the selectivity to DHP varied with time on stream. On the other hand, Pt/Al<sub>2</sub>O<sub>3</sub> and Pd/Al<sub>2</sub>O<sub>3</sub> showed low selectivity to DHP in H<sub>2</sub> flow because hydrogenation to tetrahydropyran proceeded (Table 3), and mass balance was low because of gasification.

Pt supported on acidic catalysts such as sulfated ZrO<sub>2</sub> shows a stable activity in the isomerization of alkane [36–38]. Unfortunately, noble metals such as Pt, Rh, and Pd are insufficient for keeping stable catalytic activity in H<sub>2</sub> flow. The by-products were tetrahydropyran, tetrahydrofuran, 1-pentanol, and 1-butanol in H<sub>2</sub> flow over the catalysts. In addition, over Rh/Al<sub>2</sub>O<sub>3</sub> and Pd/Al<sub>2</sub>O<sub>3</sub>, δ-valerolactone was produced at 300 °C, and 1,5-pentandiol was detected in H<sub>2</sub> flow at a low temperature of 250 °C.

In contrast to the noble metals, CuO/Al<sub>2</sub>O<sub>3</sub> showed stable conversion and high selectivity to DHP in H<sub>2</sub> flow, while it was deteriorated in N<sub>2</sub> flow (Fig. 5D). The by-products were tetrahydropyran and δ-valerolactone with a small amount produced even in H<sub>2</sub> flow. Mass balance in H<sub>2</sub> flow over CuO/Al<sub>2</sub>O<sub>3</sub> was as high as that of Rh/Al<sub>2</sub>O<sub>3</sub>. Judging from the results of TPR (Fig. 3), it is

**Table 2**  
Dehydration of THFA over metal oxide catalysts in nitrogen flow.<sup>a</sup>

Catalyst	Temperature (°C)	Conversion (%)	Selectivity (mol%)				
			DHP	THP	DVL	Others	Unrecovered
Al <sub>2</sub> O <sub>3</sub>	300	85.2	71.8	0.3	0.3	4.5	23.1
t-ZrO <sub>2</sub>	350	85.9	71.0	0.3	0.6	5.1	23.1
m-ZrO <sub>2</sub>	350	17.4	7.9	0.2	1.9	31.2	58.7
TiO <sub>2</sub>	350	47.5	27.7	0.2	0.4	7.6	64.1
Yb <sub>2</sub> O <sub>3</sub>	300	16.6	0	0	0	7.4	92.6
La <sub>2</sub> O <sub>3</sub>	300	7.2	0	0	0	78.7	21.3

THFA, tetrahydrofurfuryl alcohol; DHP, 3,4-2H-dihydropyran; THP, tetrahydropyran; DVL, δ-valerolactone. Others contain several unidentified products. Unrecovered products include gases and polymer products.

<sup>a</sup> Reaction conditions were the same as those described in Section 2. Conversion and selectivity are the average of 1 h and 5 h.

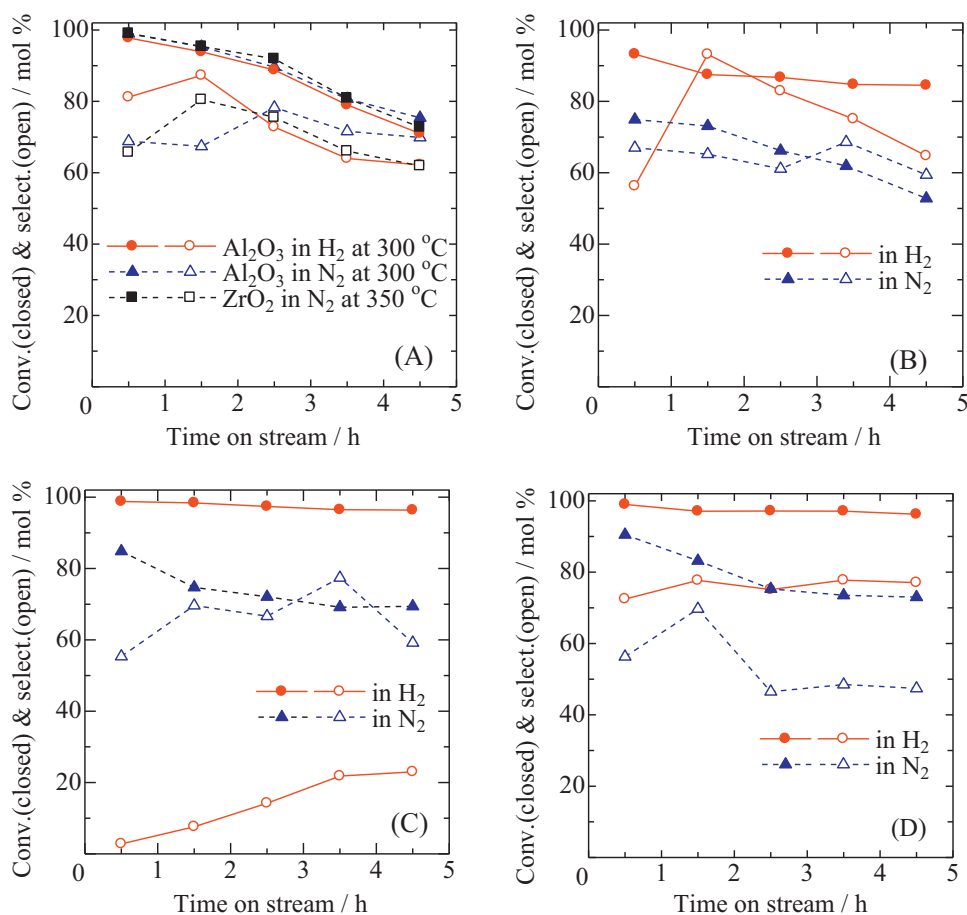


**Fig. 5.** Change in THFA conversion and DHP selectivity in different carrier gases with time on stream. (A)  $\text{Al}_2\text{O}_3$  and  $\text{ZrO}_2$ , (B) 0.5 wt.%  $\text{Rh}/\text{Al}_2\text{O}_3$ , (C) 0.5 wt.%  $\text{Pd}/\text{Al}_2\text{O}_3$ , and (D) 15 wt.%  $\text{CuO}/\text{Al}_2\text{O}_3$ . Reaction was performed at 300 °C except for  $\text{ZrO}_2$  at 350 °C. Other conditions were the same as those described in Section 2.

obvious that Cu species are reduced to metallic state, which could be maintained during the reaction in  $\text{H}_2$  flow.

Table 4 shows the effect of CuO content of  $\text{Al}_2\text{O}_3$ -supported catalysts on the reaction of THFA in  $\text{H}_2$  flow at 300 °C. The THFA conversion was almost constant irrespective of CuO content or might gradually increase with increasing CuO content. On the other hand, the selectivity to DHP seems to be maximized at CuO content of 5–10 wt.%: mass balance in this CuO range was better than that at high CuO contents as well as that at low contents.

Fig. 6 depicts the change in catalytic activity of  $\text{NiO}/\text{Al}_2\text{O}_3$  and  $\text{Co}_3\text{O}_4/\text{Al}_2\text{O}_3$  in  $\text{H}_2$  flow with time on stream, together with that of  $\text{CuO}/\text{Al}_2\text{O}_3$ . Table 3 also lists their average activity.  $\text{NiO}/\text{Al}_2\text{O}_3$  and

$\text{Co}_3\text{O}_4/\text{Al}_2\text{O}_3$  had a similar catalytic behavior to those of  $\text{Pt}/\text{Al}_2\text{O}_3$  and  $\text{Pd}/\text{Al}_2\text{O}_3$ : mass balance was low because of gasification. The by-products were tetrahydropyran, tetrahydrofuran, 1-pentanol, 1-butanol, and  $\delta$ -valerolactone in  $\text{H}_2$  flow over  $\text{NiO}/\text{Al}_2\text{O}_3$  catalyst, while the by-products over  $\text{Co}_3\text{O}_4/\text{Al}_2\text{O}_3$  catalyst were tetrahydropyran, tetrahydrofuran, and  $\delta$ -valerolactone.

### 3.4. Characterization of alumina used in the reaction

Fig. 7 shows TG-DTA profiles of pure  $\text{Al}_2\text{O}_3$  and 5 wt.%  $\text{CuO}/\text{Al}_2\text{O}_3$  catalysts used in the reaction in  $\text{H}_2$  flow at 300 °C for 5 h. A large weight loss was observed at temperatures of 200–500 °C and

**Table 3**  
Catalytic dehydration of THFA over alumina-supported catalysts in  $\text{H}_2$  at 300 °C.<sup>a</sup>

Metal or metal oxide	(content wt.%)	Conversion (%)	Selectivity (mol%)				
			DHP	THP	DVL	Others	Unrecovered
None	(0)	85.2	71.8	0.3	0.3	4.5	23.1
Rh	(0.5)	85.9	79.0	1.5	0.2	5.2	14.1
Rh	(0.5)	63.5 (in $\text{N}_2$ )	63.6	0.5	0.3	4.7	31.0
Pd	(0.5)	97.2	16.7	23.0	0	12.1	48.2
Pd	(0.5)	71.3 (in $\text{N}_2$ )	68.2	0.6	0.1	3.9	27.2
Pt	(0.5)	95.6	10.9	20.5	0	21.1	47.6
$\text{Co}_3\text{O}_4$	(15)	79.8	36.2	1.7	1.1	11.3	49.7
$\text{NiO}$	(15)	95.0	36.4	5.6	0.3	13.1	44.6
$\text{CuO}$	(15)	96.9	76.9	0.8	0.3	3.6	18.4

Abbreviations are the same as those in Table 2. Others contain tetrahydrofuran, 1-butanol, 1-pentanol, 1,5-pentanediol and unidentified products. Unrecovered products include gases and polymer products.

<sup>a</sup> Reaction conditions were the same as those described in Section 2. Conversion and selectivity are the average of 1 h and 5 h.

**Table 4**  
Catalytic dehydration of THFA over Al<sub>2</sub>O<sub>3</sub>-supported CuO catalysts in H<sub>2</sub> flow at 300 °C.<sup>a</sup>

CuO loading (wt.%)	Conversion (%)	Selectivity (mol%)				
		DHP	THP	DVL	Others	Unrecovered
0	83.2	71.6	0.3	0.2	4.4	23.6
2	93.7	72.1	0.4	0.3	3.8	23.4
5	92.3	85.4	0.7	0.2	3.3	10.4
10	88.7	86.4	0.4	0.2	4.8	8.1
15	96.9	76.9	0.8	0.3	3.5	18.4
20	99.1	78.2	0.7	0.3	2.9	17.9

Abbreviations are the same as those in Table 2. Others contain unidentified products.

<sup>a</sup> Reaction conditions were the same as those described in Section 2. Conversion and selectivity are the average of 1 h and 5 h.

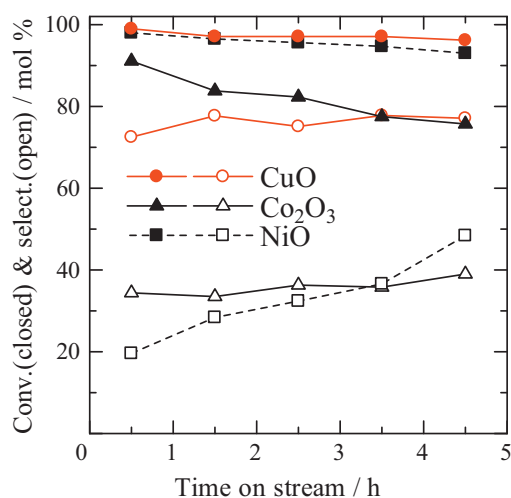


**Fig. 6.** Change in THFA conversion and DHP selectivity in H<sub>2</sub> flow at 300 °C with time on stream over 15 wt.% CuO/Al<sub>2</sub>O<sub>3</sub> (circle), 15 wt.% Co<sub>2</sub>O<sub>3</sub>/Al<sub>2</sub>O<sub>3</sub> (triangle) and 15 wt.% NiO/Al<sub>2</sub>O<sub>3</sub> (square) catalysts. Reaction conditions were the same as those of described in Section 2.

180–450 °C in the samples of Al<sub>2</sub>O<sub>3</sub> and CuO/Al<sub>2</sub>O<sub>3</sub>, respectively. The alumina used in the reaction had a weight loss of 14.5% in the TG profile at 500 °C, while the fresh alumina had a weight loss of dehydration with 3.0%. The difference of the weight loss between fresh and used catalysts would be regarded as carbon deposited on the samples during the reaction. The carbon was exothermically removed in air at 330 and 440 °C (Fig. 7), and the color of the used alumina turned white after TG analysis. The CuO/Al<sub>2</sub>O<sub>3</sub> used in the reaction, however, had a weight loss with 11.8% at 500 °C and

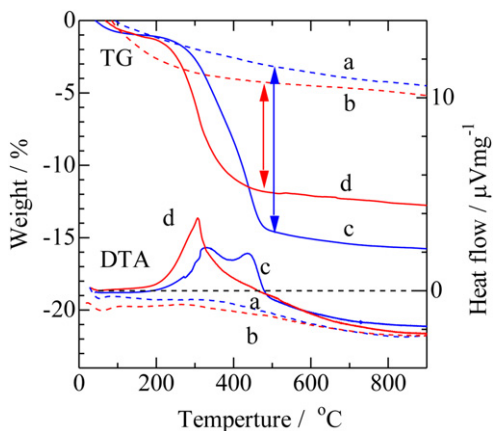


**Fig. 7.** TG-DTA profiles of Al<sub>2</sub>O<sub>3</sub> and CuO/Al<sub>2</sub>O<sub>3</sub> samples in air. (a) fresh Al<sub>2</sub>O<sub>3</sub>, (b) fresh 5 wt.% CuO/Al<sub>2</sub>O<sub>3</sub>, (c) Al<sub>2</sub>O<sub>3</sub> used in the reaction, and (d) 5 wt.% CuO/Al<sub>2</sub>O<sub>3</sub> catalyst used in the reaction. The reaction of THFA was performed in H<sub>2</sub> flow at 300 °C for 1 h.

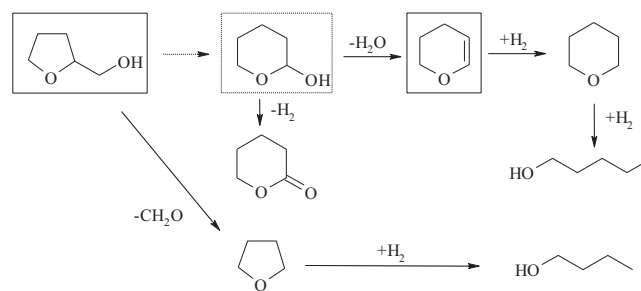


**Fig. 8.** Probable reaction routes in the reaction of THFA over alumina catalyst. 2-Hydroxytetrahydropyran was not detected in the THFA conversion at 300 °C.

exothermic peak at 300 °C, while the fresh CuO/Al<sub>2</sub>O<sub>3</sub> had a weight loss of dehydration with 4.1%. The weight loss in the removed carbonaceous materials can be estimated by the difference of the weight loss between fresh and used catalysts: the amounts of coke deposited on pure Al<sub>2</sub>O<sub>3</sub> and CuO/Al<sub>2</sub>O<sub>3</sub> are 11.5 and 7.7%, respectively. This indicates that the coke formation is inhibited in the reaction over CuO/Al<sub>2</sub>O<sub>3</sub> under H<sub>2</sub> atmosphere conditions.

### 3.5. Probable reaction route over alumina

In order to prove an intermediate species, 2-hydroxytetrahydropyran (2HTHP) was prepared as an intermediate candidate. When 2HTHP, instead of THFA, was fed into the reactor over Cu-alumina catalyst in H<sub>2</sub> at 200 °C, 2HTHP was converted to DHP and to  $\delta$ -valerolactone with the selectivity of 64 and 10%, respectively, at 100% conversion. The other products were 1-pentanol, pentanoic acid, and 1,5-pentanediol. Therefore, 2HTHP can be readily dehydrated to DHP at a temperature lower than 300 °C which is the effective reaction temperature of THFA. It is proposed that 2HTHP is probably an intermediate from THFA to DHP.

Fig. 8 summarizes a probable reaction routes in the conversion of THFA over modified alumina catalysts. At 300 °C, THFA could be rearranged into 2HTHP. 2HTHP is immediately dehydrated to DHP, so that it could not be detected in the effluent mixture. Thus, the rate determining step is probably the initial step, which is the rearrangement of THFA into 2HTHP. The major by-products such as tetrahydropyran and  $\delta$ -valerolactone are formed through step-wise hydrogenation of DHP and dehydrogenation of 2HTHP, respectively. Over the catalysts with high potential in hydrogenation and hydrogenolysis, 1-pentanol, tetrahydrofuran, and 1-butanol are formed via step-wise reactions, as shown in Fig. 8.

## 4. Conclusions

Vapor-phase catalytic conversion of THFA to produce DHP was investigated over acidic catalysts modified with transition metals. Catalytic activity of alumina was seriously deactivated in N<sub>2</sub> flow

at 300 °C, whereas the initial activity was high. Tetragonal ZrO<sub>2</sub> also showed the same catalytic activity as alumina at 350 °C. The catalytic activity of alumina modified with either Cu or Rh was stabilized in the conversion of THFA into DHP under H<sub>2</sub> flow conditions. The optimum activity was obtained in the catalysts at CuO contents of 5–10 wt.%; the selectivity to DHP exceeded 85% and the best mass balance was achieved. CuO was reduced to metallic Cu that was maintained during the reaction at 300 °C, Cu metal probably works as a remover for deposited carbon and prevents coke formation by the aid of hydrogen. In the conversion of THFA to DHP, we propose that THFA is initially rearranged into 2-hydroxytetrahydropyran as an intermediate that is rapidly dehydrated to DHP. The first-step rearrangement could be the rate-determining step in the reaction.

## References

- [1] J.J. Bozell, G.R. Petersen, *Green Chem.* 12 (2010) 539–554.
- [2] A. Singh, K. Das, D.K. Sharma, *J. Chem. Technol. Biotechnol.* 34A (1984) 51–61.
- [3] F.W. Lichtenthaler, *Carbohydr. Res.* 313 (1998) 69–89.
- [4] D. Montané, J. Salvadó, C. Torras, X. Farriol, *Biomass Bioenergy* 22 (2002) 295–304.
- [5] C. Moreau, R. Durand, D. Peyron, J. Duhamet, P. Rivalier, *Ind. Crops Prod.* 7 (1998) 95–99.
- [6] J. Zhang, J. Zhuang, L. Lin, S. Liu, Z. Zhang, *Biomass Bioenergy* 39 (2012) 73–77.
- [7] O.W. Cass, *Ind. Eng. Chem.* 40 (1948) 216–219.
- [8] A. Corma, S. Iborra, A. Velty, *Chem. Rev.* 107 (2007) 2411–2502.
- [9] J.N. Chheda, G.W. Huber, J.A. Dumesic, *Angew. Chem. Int. Ed.* 46 (2007) 7164–7183.
- [10] M. Hronec, K. Fulajtarová, *Catal. Commun.* 24 (2012) 100–104.
- [11] N. Merat, C. Godawa, A. Gaset, *J. Chem. Technol. Biotechnol.* 48 (1990) 145–159.
- [12] H.P. Thomas, C.L. Wilson, *J. Am. Chem. Soc.* 73 (1951) 4803–4805.
- [13] H.-Y. Zheng, Y.-L. Zhua, B.-T. Teng, Z.-Q. Bai, C.-H. Zhang, H.-W. Xiang, Y.-W. Li, *J. Mol. Catal. A: Chem.* 246 (2006) 18–23.
- [14] W.H. Bagnall, E.P. Goodings, C.L. Wilson, *J. Am. Chem. Soc.* 73 (1951) 4794–4798.
- [15] E.P. Goodings, C.L. Wilson, *J. Am. Chem. Soc.* 73 (1951) 4798–4800.
- [16] E.P. Goodings, C.L. Wilson, *J. Am. Chem. Soc.* 73 (1951) 4801–4802.
- [17] R.L. Sawyer, D.W. Andrus, *Org. Synth.* 23 (1943) 25; R.L. Sawyer, D.W. Andrus, *Org. Synth. Coll.* 3 (1955) 276.
- [18] L.E. Schniepp, H.H. Geller, *J. Am. Chem. Soc.* 68 (1946) 1646–1648.
- [19] C.L. Wilson, *J. Am. Chem. Soc.* 69 (1947) 3004–3006.
- [20] The Quaker Oats Co., GB Patent 858626 (1959).
- [21] W.J. Gensler, G.L. Mcleod, *J. Org. Chem.* 28 (1963) 3194–3197.
- [22] Olin Mathieson Chemical Co., GB Patent 1017313 (1963).
- [23] J. Schoeder, K. Ebel, BASF, EP Patent 0691337 (1996).
- [24] H. Weigl, K. Ebel, J. Simon, BASF AG, WO 02/12219 (2002).
- [25] Y.V.S. Rao, S.J. Kulkarni, M. Subrahmanyam, A.V.R. Rao, *J. Org. Chem.* 59 (1994) 3998–4000.
- [26] X. Jiang, Z. Shen, *J. Wuhan Univ. Technol.* 20 (2005) 92–94.
- [27] D. Kaufman, W. Reeve, *Org. Syn.* 26 (1946) 83; D. Kaufman, W. Reeve, *Org. Syn. Coll. Vol.* 3 (1955) 693.
- [28] M. Schlaf, *Dalton Trans.* (2006) 4645–4653.
- [29] S. Koso, I. Furikado, A. Shimao, T. Miyazawa, K. Kunimori, K. Tomishige, *Chem. Commun.* (2009) 2035–2037.
- [30] S. Koso, Y. Nakagawa, K. Tomishige, *J. Catal.* 280 (2011) 221–229.
- [31] Y. Nakagawa, K. Tomishige, *Catal. Today* 195 (2012) 136–143.
- [32] S. Sato, R. Takahashi, N. Yamamoto, E. Kaneko, H. Inoue, *Appl. Catal. A: Gen.* 334 (2008) 84–91.
- [33] F. Sato, H. Okazaki, S. Sato, *Appl. Catal. A: Gen.* 419–420 (2012) 41–48.
- [34] F. Sato, S. Sato, *Catal. Commun.* 27 (2012) 129–133.
- [35] A.C. Ott, M.F. Murray, R.L. Pederson, *J. Am. Chem. Soc.* 74 (1952) 1239–1241.
- [36] H. Hattori, *Top. Catal.* 53 (2010) 432–438.
- [37] T. Shishido, H. Hattori, *J. Catal.* 161 (1996) 194–197.
- [38] K. Tomishige, A. Okabe, K. Fujimoto, *Appl. Catal. A: Gen.* 194 (2000) 383–393.
- [39] S. Sato, N. Sato, Y. Yamada, *Chem. Lett.* 41 (2012) 831–833.
- [40] K. Kojima, M. Kimura, S. Ueda, Y. Tamaru, *Tetrahedron* 62 (2006) 7512–7520.
- [41] S. Sato, R. Takahashi, T. Sodesawa, A. Igarashi, H. Inoue, *Appl. Catal. A* 328 (2007) 109–116.
- [42] S. Sato, R. Takahashi, M. Kobune, H. Gotoh, *Appl. Catal. A* 356 (2009) 57–63.